Changes in Expression of Receptor-Interacting Protein Kinase 1 in Secondary Neural Tissue Damage Following Spinal Cord Injury

Haruo Kanno[1] (iD), Hiroshi Ozawa[2], Kyoichi Handa[1], Taishi Murakami[1] and Eiji Itoi[1]

[1]Department of Orthopaedic Surgery, Tohoku University Graduate School of Medicine, Sendai, Japan. [2]Department of Orthopaedic Surgery, Tohoku Medical and Pharmaceutical University, Sendai, Japan.

ABSTRACT

INTRODUCTION: Necroptosis is a form of programmed cell death that is different from apoptotic cell death. Receptor-interacting protein kinase 1 (RIPK1) plays a particularly important function in necroptosis execution. This study investigated changes in expression of RIPK1 in secondary neural tissue damage following spinal cord injury in mice. The time course of the RIPK1 expression was also compared with that of apoptotic cell death in the lesion site.

METHODS AND MATERIALS: Immunostaining for RIPK1 was performed at different time points after spinal cord injury. The protein expressions of RIPK1 were determined by western blot. The RIPK1 expressions in various neural cells were investigated using immunohistochemistry. To investigate the time course of apoptotic cell death, TUNEL-positive cells were counted at the different time points. To compare the incidence of necroptosis and apoptosis, the RIPK1-labeled sections were co-stained with TUNEL.

RESULTS: The RIPK1 expression was significantly upregulated in the injured spinal cord. The upregulation of RIPK1 expression was observed in neurons, astrocytes, and oligodendrocytes. The increase in RIPK1 expression started at 4 hours and peaked at 3 days after injury. Time course of the RIPK1 expression was similar to that of apoptosis detected by TUNEL. Interestingly, the increased expression of RIPK1 was rarely observed in the TUNEL-positive cells. Furthermore, the number of RIPK1-positive cells was significantly higher than that of TUNEL-positive cells.

CONCLUSIONS: This study demonstrated that the expression of RIPK1 increased in various neural cells and peaked at 3 days following spinal cord injury. The temporal change of the RIPK1 expression was analogous to that of apoptosis at the lesion site. However, the increase in RIPK1 expression was barely seen in the apoptotic cells. These findings suggested that the RIPK1 might contribute to the pathological mechanism of the secondary neural tissue damage after spinal cord injury.

KEYWORDS: Spinal cord injury, necroptosis, receptor-interacting protein kinase 1, cell death, necrosis, apoptosis

Introduction

Necroptosis is a form of programmed cell death that is different from apoptotic cell death, which is mediated by a caspase-dependent pathway.[1] The DNA fragmentation in the nuclei induced by caspase activation is not observed in necroptosis.[2] Necroptosis has the morphological characteristics of necrotic cell death, such as cell swelling and membrane rupture, but not those of apoptosis, which include chromatin condensation, nuclear shrinkage, and fragmentation.[3] Previous studies have demonstrated that the receptor-interacting protein kinase (RIPK) specifically regulates necroptosis.[1,3] The RIPK1 expression increases in various models of central nervous system (CNS) disease, including intracerebral hemorrhage,[4] neonatal brain hypoxia/ischemia,[5] and traumatic brain injury.[6] In addition, the inhibition of RIPK1 provides a neuroprotective effect in various CNS diseases.[4,7-9] Recently, it was also reported that RIPK1 has an important role in inflammation in various disease models.[10,11]

It has been considered that secondary neural tissue damage following spinal cord injury (SCI) is mainly induced by apoptotic cell death. Previous studies that have investigated cell death after SCI have mostly focused on apoptosis, but not necroptosis. Only a few studies have suggested that the inhibition of RIPK1 reduced the neural tissue damage after SCI.[12,13] To our knowledge, there have been no studies to investigate the time course of the RIPK1 protein expression in damaged neural tissue following SCI. Whether the time course of the RIPK1 expression differs from that of apoptosis—which is conventionally considered to be the main cause of secondary tissue damage—has also been unknown.

This study examined the temporal change in the RIPK1 protein expression in damaged neural tissue after SCI in mice.

The time course of the RIPK1 expression was also compared with that of apoptotic cell death in the lesion site.

Materials and Methods

Mice

Adult female C57BL/6J mice aged 8 to 10 weeks (Charles River, Japan Inc, Yokohama, Japan) were used in the experiments of this study. All experimental procedures were approved by the Institutional Animal Care and Use Committee of Tohoku University. All efforts were made to minimize the number of animals used and to reduce their suffering.

Surgical procedures

All surgical procedures were performed under general anesthesia with 2% sevoflurane. Using an operating microscope, laminae were exposed at T9-T11 level. Laminectomy was performed at T10 level and exposed the dorsal surface of the spinal cord without disrupting the dura mater. The entire left hemicord at T10 was transected using a sharp scalpel.[14,15] The sham-operated animals underwent the same surgery, although hemisection of the cord was not applied.

Preparation of tissue sections

At the defined survival times (4 hours, 24 hours, 3 days, 7 days, and 21 days) following spinal cord hemisection, the mice were transcardially perfused with 0.9% saline, followed by 4% paraformaldehyde. After perfusion, the spinal cord segments containing the injured site were removed and postfixed in the same fixative solution for 24 hours at 4°C. Then, these tissues were cryoprotected in 30% sucrose in phosphate-buffered saline (PBS) for 48 hours at 4°C and embedded in Optimal-Cutting-Temperature compound (Sakura Finetek, Tokyo, Japan). Serial 15-μm transverse cryostat sections obtained from around the injured site were mounted on slides and then stored at −20°C until use. A total of 13 sequential sections were collected at 250-μm intervals that spanned 3000 μm in length along the spinal cord, centered at the epicenter.

Immunostaining of RIPK1

The spinal cord sections were washed in PBS for 15 minutes. Then, the sections were incubated with PBS containing 0.3% Triton X-100 for 10 minutes and blocked with 3% milk and 5% fetal bovine serum (FBS) in 0.01 M PBS for 2 hours to avoid nonspecific staining. The sections were incubated with primary antibody against mouse RIPK1 (1:100; BD Transduction Laboratories, San Jose, CA, USA) diluted in PBS overnight at 4°C, followed by secondary antibodies. The stained sections were coverslipped with VECTASHIELD containing DAPI (4′,6-diamidino-2-phenylindole) to label the nuclei (Vector Laboratories, Burlingame, CA, USA). Then each section was scanned using a fluorescence microscope (BX 51; Olympus, Tokyo, Japan). The immunostaining was performed at the same time in each experiment.

RIPK1-positive cell counting

To evaluate the protein expression of RIPK1 in the spinal cord, the number of RIPK1-positive cells in the injured and contralateral sides of the spinal cord was counted using serial transverse sections at 250-μm intervals. The scanned image of the stained section was displayed on a monitor with a grid using the Photoshop CS4 (Adobe, San Jose, CA, USA) and then RIPK1-positive cells were counted using a manual counter. The sections with the highest number of RIPK1-positive cells on the injured side and the 250-μm rostral and caudal sections in each animal were selected for the analysis. The sum of the numbers in the 3 sections was determined and then compared among the injured side, the contralateral side, and the sham group.[14,16]

Western blotting of RIPK1

At 3 days after hemisection of the spinal cord, the animals were sacrificed to obtain the spinal cord tissues. The T10 spinal cord segment (3 mm length) centered at the injured site was removed and then homogenized in lysis buffer containing 50 mM Tris HCl (pH 7.6), 20 mM $MgCl_2$, 150 mM NaCl, 0.5% Triton-X, 5 units/mL aprotinin, 5 μg/mL leupeptin, 5 μg/mL pepstatin, 1 mM benzamidine, and 1 mM phenylmethylsulfonyl fluoride. Following centrifugation at 12 000 rpm, 4°C for 15 minutes, the protein levels in the supernatant were determined using the Bradford assay (Bio-Rad Laboratories, Hercules, CA, USA). Then, the samples (30 μg) were subjected to sodium dodecyl sulfate–polyacrylamide gel electrophoresis (SDS-PAGE) in 15% gels and then electrophoretically transferred to a polyvinylidene difluoride filter (PVDF) membranes. The membranes were blocked with TBST buffer (0.01 M Tris HCl, pH 7.5, 0.15 M NaCl, and 0.05% Tween 20) containing 3% milk for 1 hour and incubated with mouse anti-RIPK1 antibodies (1:100; BD Transduction Laboratories) overnight. After washing with TBST, the membranes were incubated with secondary antibodies (1:1000; Invitrogen, Toyko, Japan) for 2 hours at room temperature. The blots were detected using an enhanced chemiluminescence (ECL) kit (Amersham Corp, Burlington, MA, USA). The band density was quantified using a scanned densitometric analysis and the Image Lab software program (version 4.1; Bio-Rad Laboratories) and normalized according to the level of β-tubulin. The protein level of RIPK1 was compared between the injured and the uninjured spinal cord samples.

Double-staining for RIPK1 and markers of various cell types

To examine the RIPK1 expression in a specific population of cells, the spinal cord sections obtained at 3 days were double-stained for RIPK1 and markers of various neural cell types: NeuN for neurons, glial fibrillary acidic protein (GFAP) for astrocytes, and Olig2 for oligodendrocytes. After rinsing the sections with PBS, they were incubated with PBS containing

0.3% Triton X-100 for 10 minutes and blocked with 3% milk and 5% FBS in 0.01 M PBS for 2 hours to avoid nonspecific staining. The sections were incubated with a mixture of rabbit anti-RIPK1 antibody (1:100; Santa Cruz Biotechnology, Dallas, TX) and either goat anti-Olig2 (1:100; Santa Cruz Biotechnology), mouse anti-GFAP (1:50; Dako, Tokyo, Japan), or mouse anti-NeuN (1:100; Chemicon, Temecula, CA, USA) antibodies diluted in PBS overnight at 4°C. The sections were washed with PBS and then incubated with secondary antibodies. The stained section was mounted with VECTASHIELD containing DAPI (Vector Laboratories). The specificity of the RIPK1 antibody was confirmed by omission of the primary antibody in this protocol to abrogate the immunoreactive staining.[17,18]

TUNEL

To investigate the time course of apoptosis in the injured spinal cord, terminal deoxynucleotidyl transferase–mediated dUTP nick end labeling (TUNEL) was applied to sections at different time points after injury using an In Situ Cell Death Detection Kit (Roche Diagnostics, Basel Switzerland). The labeled sections were mounted with VECTASHIELD containing DAPI to label the nuclei (Vector Laboratories) and scanned with a fluorescence microscope (BX 51; Olympus). TUNEL-positive cells were defined as cells that were double-labeled with TUNEL and DAPI. Using serial transverse sections at 250-μm intervals, the number of TUNEL-positive cells was counted in the injured and contralateral sides. The sections with the highest number of TUNEL-positive cells on the injured side and the 250-μm rostral and caudal sections were selected in each animal. The sum of the numbers in the 3 sections was calculated and compared among the injured side, the contralateral side, and the sham control.

Double-staining of RIPK1 and TUNEL

To compare the number of RIPK1-expressing cells and apoptotic cells characterized by DNA fragmentation, double-staining of RIPK1 and TUNEL was performed using spinal cord sections at 3 days following injury. Based on the evaluation of TUNEL, as described above, the serial sections with the highest number of TUNEL-positive cells on the injured side and the 250-μm rostral and caudal sections in each animal were selected and used for this analysis. After immunostaining of RIPK1, as described above, TUNEL was performed. Then, the sum of the number of TUNEL-positive and/or RIPK1-positive cells was compared in the 3 sections of the injured side.

Statistical analysis

Significant differences in the number of RIPK1-positive and TUNEL-positive cells in the cell counting were determined using a mixed-model analysis of variance (ANOVA) followed by the Tukey-Kramer post hoc test. In the western blot analysis, statistical difference in the band density was analyzed using an unpaired t-test. P-value less than .05 was considered to be statistically significant. Data were as represented as mean ± SD.

Results

Temporal expression of RIPK1 in the spinal cords following injury

In immunostaining of RIPK1, the uninjured cords showed no obvious expression of RIPK1 (Figure 1). In contrast, the cells expressing RIPK1 increased on the injured side of the spinal cord (Figure 1). On the injured side, the cells expressing RIPK1 were observed in both the gray and the white matter of the spinal cord. RIPK1 was not expressed by all of the cells on the injured side. The RIPK1-expressing cells were rarely observed on the contralateral side, similar to the sham group.

In representative pictures of RIPK1 staining at different time points (Figure 2A), the population of RIPK1-expressing cells on the injured side increased at 24 hours and 3 and 7 days compared with the other time points. In the counting of RIPK1-positive cells (Figure 2B), the number of RIPK1-positive cells on the injured side was significantly higher than that on the contralateral side and in the sham group ($P < .05$). A significant increase in the number of RIPK1-positive cells was first noted at 24 hours and lasted for 7 days. The maximum number of RIPK1-positive cells on the injured side was observed at 3 days after injury. Western blot analysis revealed that the protein expression of RIPK1 in the injured spinal cord was higher than that in the uninjured cord (Figure 2C). The analysis of band density revealed that the RIPK1 expression significantly increased in the injured spinal cord ($P < .05$).

The expression of RIPK1 increased in various neural cells at lesion site

To investigate the RIPK1 expression in specific population of neural cells, spinal cord sections obtained at 3 days after injury were double-stained for RIPK1 and markers of various neural cell types. On double-staining, the expression of RIPK1 was observed in the NeuN-, GFAP-, and Olig2-labeled cells (Figure 3). The double-staining indicated that RIPK1 actually expressed in neurons, astrocytes, and oligodendrocytes although not all of these cells expressed RIPK1.

Temporal change in the RIPK1 expression coincided with apoptosis

Using TUNEL-stained sections obtained at different time points, the time course of apoptosis in the injured spinal cord was evaluated. In representative pictures, the number of TUNEL-positive cells on the injured side after hemisection increased in comparison with the number observed in the sham group (Figure 4A). The number of TUNEL-positive cells on the injured side at 24 hours and 3 days were relatively higher in
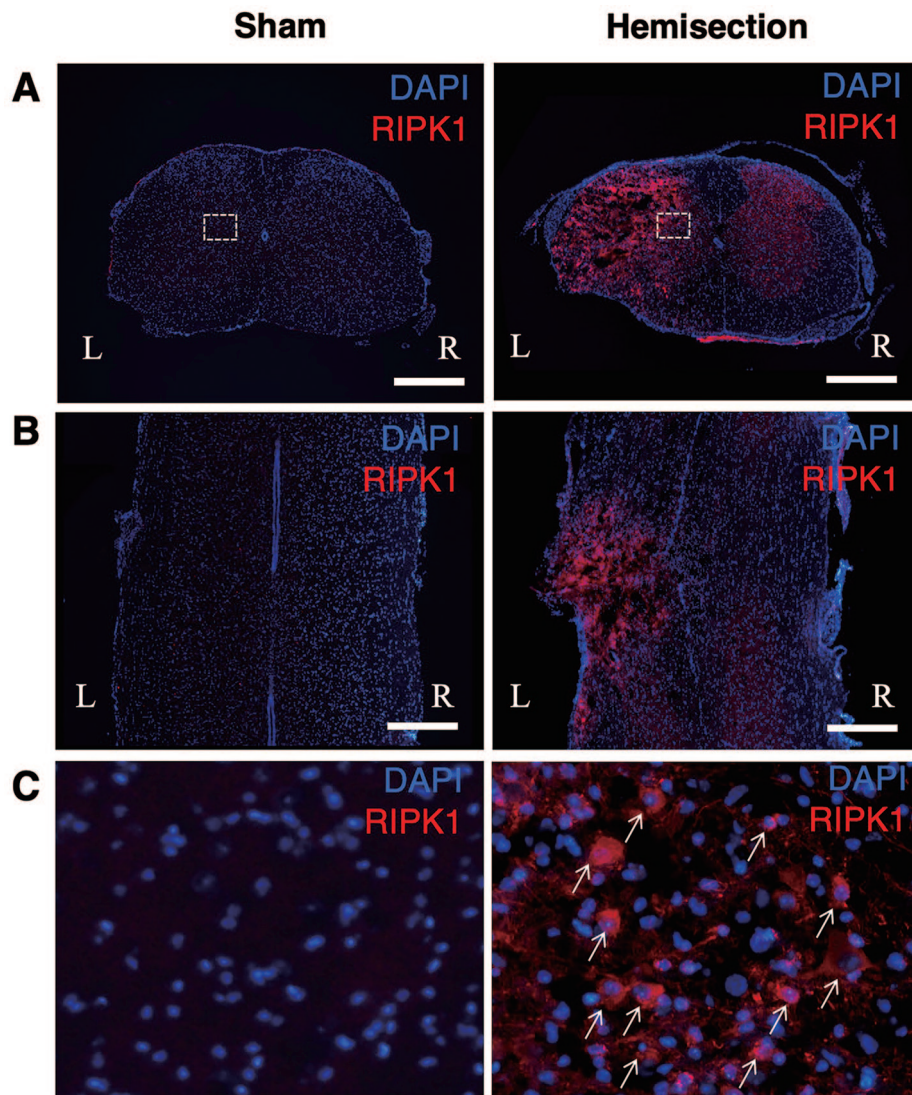
Figure 1. Upregulation of RIPK1 expression in the spinal cords after hemisection. Immunostaining of RIPK1 reveals that the uninjured cords showed no obvious expression of RIPK1 in the transverse (A) and horizontal (B) sections. At 3 days after the hemisection, the RIPK1 expression on the injured side (L) increased compared with that on the contralateral side (R) in the transverse (A) and horizontal (B) sections. Scale bars: 500 μm. High-magnification views (C) of boxed areas in (A). RIPK1-positive cells (arrows) increased at the lesion site (C). RIPK1 indicates receptor-interacting protein kinase 1.

comparison with the number observed at other time points. The counting of the TUNEL-positive cells revealed that the number of TUNEL-positive cells on the injured side was significantly higher than the number observed on the contralateral side and in the sham control group (Figure 4B). A significant increase in the number of TUNEL-positive cells was observed at 24 hours and 3 days after injury ($P < .05$). Same as the RIPK1-positive cells, the maximum number of TUNEL-positive cells was observed at 3 days and it thereafter decreased at 7 days following injury.

In double-staining of RIPK1 and TUNEL (Figure 4C to F), the populations of TUNEL-positive and RIPK1-positive cells were observed to be increased on the injured side (Figure 4C and D). Interestingly, the increased expression of RIPK1 was rarely observed in the TUNEL-positive cells (Figure 4C and D). The high-magnification image demonstrated that most of the TUNEL-positive cells having fragmented or shrunken nuclei, as is typical of apoptotic nuclei, did not express RIPK1 (Figure 4E and F). In the counting of TUNEL-positive and RIPK1-positive cells, the number of RIPK1-positive cells was significantly higher than the number of TUNEL-positive cells (Figure 4G). The number of cells that were both TUNEL-positive and RIPK1-positive was significantly lower in comparison with the number of cells that were singularly positive for TUNEL or RIPK1 (Figure 4H).

Discussion

This study demonstrated that the expression of RIPK1 significantly increased on the injured site following spinal cord hemisection. The increased expression of RIPK1 was observed in various types of neural cells, including neurons, astrocytes, and oligodendrocytes. An increase in the number of RIPK1-positive cells was observed from 24 hours after injury; the number peaked at 3 days and remained elevated for at least
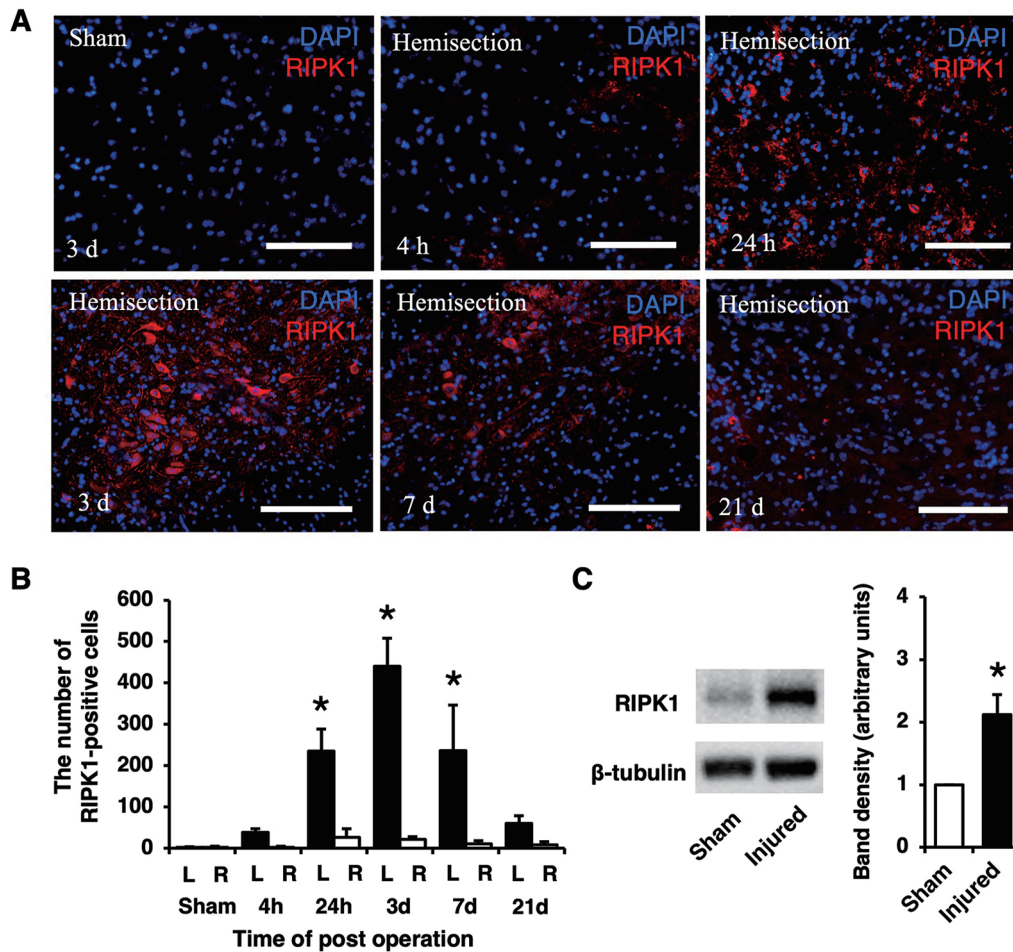
Figure 2. Immunostaining of RIPK1 on the injured side at different time points. The population of RIPK1-expressing cells at 24 hours and 3 and 7 days were larger than those at the other time points (A). Scale bars: 100 μm (A). The number of RIPK1-positive cells was significantly higher on the injured side (L) than that on the contralateral side (R) and in the sham group at 24 hours and 3 and 7 days (B). Western blotting showed that the RIPK1 protein expression increased in the injured spinal cord (C). A quantitative analysis of the band density revealed that the level of RIPK1 proteins in the injured spinal cord was significantly higher than that in the uninjured spinal cord samples. All values are presented as mean ± SD. *$P < .05$, n = 3 and 5 per each group in (B) and (C), respectively. RIPK1 indicates receptor-interacting protein kinase 1.

7 days. Notably, the time course of the RIPK1 expression in the injured spinal cord was similar to that of apoptosis detected by TUNEL. The number of RIPK1-positive cells was significantly higher than that of TUNEL-positive cells in the damaged neural tissue. The TUNEL-positive cells having fragmented or shrunken nuclei—as is typical of apoptotic nuclei—rarely expressed RIPK1. These findings suggest that RIPK1 might have a molecular function that is involved in the secondary neural tissue damage after SCI.

Not only apoptosis but also necrosis has been shown to be present in the damaged neural tissue following SCI.[19,20] Apoptosis generally occurs as a relatively delayed cell death compared with necrosis after SCI.[19] Conventionally, secondary neural tissue damage after SCI has been considered to be mainly caused by apoptotic cell death. Previous reports related to cell death in the injured spinal cord have focused on apoptosis. Previous studies have demonstrated that the time course of apoptosis causing secondary damage peaked at approximately 3 days after SCI.[19-21] Neuronal apoptosis is usually completed

within the first 24 h after SCI although glial apoptosis has been shown to persist.[22] This study demonstrated that the number of TUNEL-positive cells peaked at 3 days after injury. In addition, the increase in the expression of RIPK1 started at 24 hours, peaked at 3 days, and lasted for 7 days after injury. These findings indicate that the temporal change in the RIPK1 expression following SCI was similar to that in apoptotic cell death causing secondary damage after SCI. Recently, several studies have revealed that different phenotypes of cell death, including necroptosis, occur at the lesion site after CNS injury.[9,23] A previous study suggested that the inhibition of RIPK1 reduced secondary damage and improved functional recovery after SCI.[12] Together, these data suggest that the upregulation of the RIPK1 expression might contribute to secondary neural tissue damage following SCI.

Many previous studies showed that necroptosis can be executed in different types of neural cells and contribute to multiple pathological conditions in various CNS diseases. Necroptosis can be induced in hippocampal neurons in models
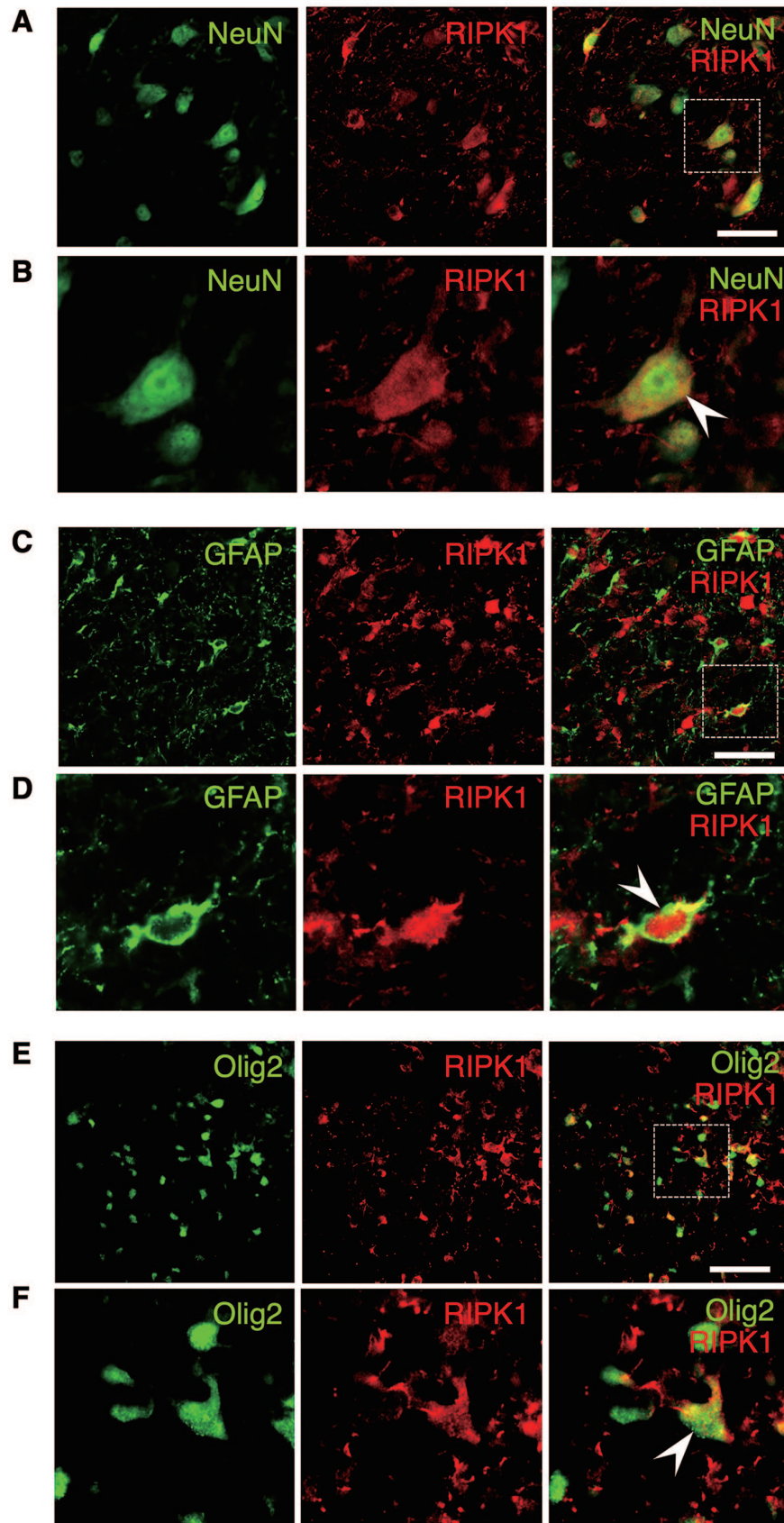
Figure 3. Double-staining for RIPK1 and markers of various neural cell types. The upregulation of RIPK1 expression was observed in the NeuN-, GFAP-, and Olig2-labeled cells (arrowhead), demonstrating that the expression of RIPK1 increased in neurons, astrocytes, and oligodendrocytes, respectively. High-magnification images of boxed areas in (A), (C), and (E) are shown in (B), (D), and (F), respectively. Scale bars: 50 μm (A, C, E). RIPK1 indicates receptor-interacting protein kinase 1.
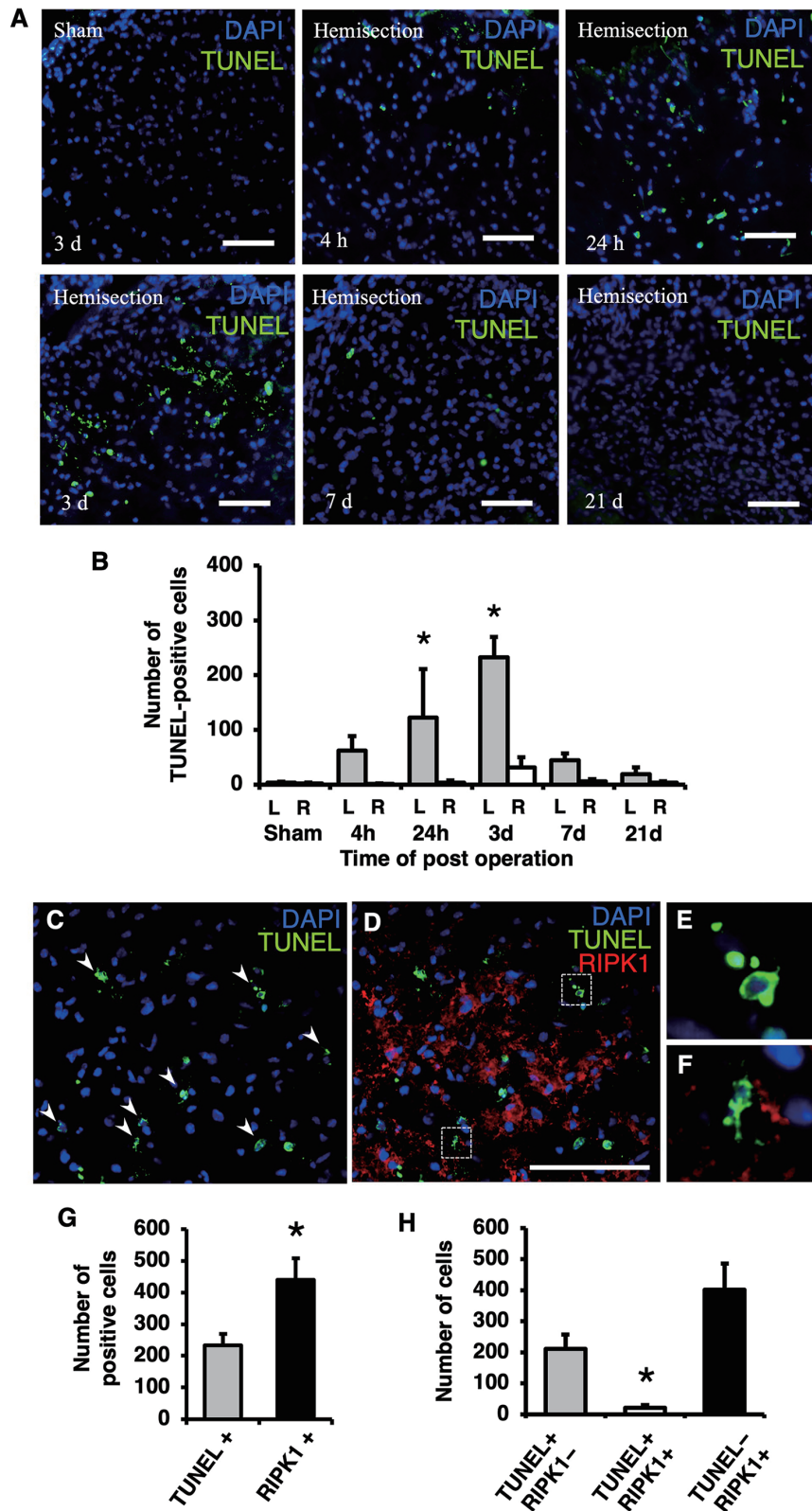
Figure 4. Comparison of TUNEL and RIPK1 staining in the injured spinal cord. TUNEL staining on the injured side at different time points following injury (A). The population of TUNEL-positive cells was larger at 24 hours and 3 days than at the other time points (A). Scale bars: 50 μm (A). The number of TUNEL-positive cells was significantly higher on the injured side (L) than the contralateral side (R) and in the sham group at 24 hours and 3 days (B). Double-staining for RIPK1 and TUNEL on the injured side at 3 days (C to F). The TUNEL-positive cells exhibiting fragmented or shrunken nuclei (arrowheads in C), a hallmark of apoptosis, rarely expressed RIPK1 (D). High-magnification views (E, F) of boxed areas in (D) show the fragmented or shrunken TUNEL-positive nuclei. Scale bars: 100 μm (D). The number of TUNEL-positive and RIPK1-positive cells on the injured side at 3 days. The number of RIPK1-positive cells was significantly higher in comparison with the number of TUNEL-positive cells (G). The number of cells that were both TUNEL-positive and RIPK1-positive was significantly lower in comparison with the number of cells that were singularly TUNEL-positive or RIPK1-positive (H). All values are presented as mean ± SD. *$P < .05$, n = 3 per each group. RIPK1 indicates receptor-interacting protein kinase 1.

of ischemic brain injury.[24] Necroptosis contributes to oligodendrocyte death in the cerebral white matter injury induced by hypoxia-ischemia in the developing brain.[25] RIPK1-mediated necroptosis contributes to neuronal and astrocytic cell death in ischemic stroke.[26] The inhibition of RIPK1 can protect oligodendrocyte precursor cells and reduce white matter injury after transient focal cerebral ischemia in mice.[27] Importantly, this study showed that the increased expression of RIPK1 was observed in neurons, astrocytes, and oligodendrocytes at the lesion site following SCI. These results suggested that necroptosis may occur in different types of neural cells and contribute to various pathological mechanisms in SCI. Further studies are needed to clarify the precise molecular and pathological mechanisms of necroptosis in the injured spinal cord.

The inhibition of RIPK1 activity was shown to reduce necroptosis and have a tissue-protective function in various disease models.[9,28] Previous studies have suggested that the inhibition of RIPK1 to attenuate necroptosis provided a therapeutic effect in CNS diseases. The inhibition of RIPK1 reduced white matter injury and improved long-term functional recovery from focal cerebral ischemia.[27] Treatment with necrostatin-1, to inhibit RIPK1 activity, reduced brain tissue damage and improved the functional outcome in a traumatic brain injury model.[8] The inhibition of RIPK1 was found to reduce necrotic cell death, inflammation, and oxidative damage following neonatal hypoxia-ischemia-induced brain injury.[5] Recent studies suggested that the inhibition of RIPK1 may reduce the neural tissue damage after SCI and therefore have therapeutic potential. The RIPK1 inhibitor Nec-1 reduces necroptosis by inhibiting RIPK1/3-mixed lineage kinase domain-like pseudokinase (MLKL) recruitment and improves the pathological condition and locomotor impairment after SCI.[12] The inhibition of RIPK1 by Nec-1 reduces necrotic cell death in astrocytes at the lesion site following SCI.[29] Notably, this study showed that the number of RIPK1-positive cells was significantly higher than that of TUNEL-positive cells in damaged neural tissue at 3 days after injury. Thus, the inhibition of RIPK1 to attenuate necroptosis may be a more effective treatment for reducing secondary damage following SCI in comparison with anti-apoptotic treatment.

There are several limitations in this study. First, the RIPK1-positive cell counting was not completed using unbiased stereology. This study used the dominant method for quantifying cell numbers histologically within the injured spinal cord. Therefore, the results of the RIPK1-positive cell counting may not directly reflect the actual change in the RIPK1 expression in the damaged neural tissue after SCI. Second, in the western blot analysis of RIPK1, the tissue samples of the spinal cords after hemisection were containing not only injured side but also contralateral side of the cord. The RIPK1 protein concentration on the injured side within the spinal cord samples should be diluted with undamaged tissue on the contralateral side. Such issue may reflect differences in the results of

increased RIPK1 expression in the injured spinal cord between the western blot and the immunohistochemistry. Third, previous studies indicated that noxious input enhances tissue damage by increasing the extent of hemorrhage and cell death following SCI.[30] Therefore, uncontrolled pain after SCI may affect the progression of secondary damage and consequently confound the results in this study.

In conclusion, the expression of RIPK1 significantly increased in the injured spinal cord. The upregulation of RIPK1 expression was observed in various neural cells including neurons, astrocytes, and oligodendrocytes. The time course of the RIPK1 expression was similar to that of apoptosis detected by TUNEL. The TUNEL-positive cells exhibiting fragmented or shrunken nuclei—as is typical of apoptotic nuclei—rarely expressed RIPK1. These findings imply that the upregulation of RIPK1 might be involved in pathological mechanism of the secondary neural tissue damage after SCI. Thus, inhibiting RIPK1 may provide a neuroprotective effect to reduce secondary damage and be a promising therapeutic strategy for SCI.

Author Contributions

ORCID iD

Haruo Kanno https://orcid.org/0000-0003-1985-2257

REFERENCES

1. Vandenabeele P, Galluzzi L, Vanden Berghe T, Kroemer G. Molecular mechanisms of necroptosis: an ordered cellular explosion. *Nat Rev Mol Cell Biol*. 2010; 11:700-714.
2. Hotchkiss RS, Strasser A, McDunn JE, Swanson PE. Cell death. *N Engl J Med*. 2009;361:1570-1583.
3. Hitomi J, Christofferson D, Ng A, et al. Identification of a molecular signaling network that regulates a cellular necrotic cell death pathway. *Cell*. 2008;135: 1311-1323.
4. Shen H, Liu C, Zhang D, et al. Role for RIP1 in mediating necroptosis in experimental intracerebral hemorrhage model both in vivo and in vitro. *Cell Death Dis*. 2017;8:e2641.
5. Northington F, Chavez-Valdez R, Graham E, Razdan S, Gauda E, Martin L. Necrostatin decreases oxidative damage, inflammation, and injury after neonatal HI. *J Cereb Blood Flow Metab*. 2011;31:178-189.
6. Zhou H, Chen L, Gao X, Luo B, Chen J. Moderate traumatic brain injury triggers rapid necrotic death of immature neurons in the hippocampus. *J Neuropathol Exp Neurol*. 2012;71:348-359.
7. Degterev A, Huang Z, Boyce M, et al. Chemical inhibitor of nonapoptotic cell death with therapeutic potential for ischemic brain injury. *Nat Chem Biol*. 2005;1:112-119.
8. You Z, Savitz S, Yang J, et al. Necrostatin-1 reduces histopathology and improves functional outcome after controlled cortical impact in mice. *J Cereb Blood Flow Metab*. 2008;28:1564-1573.
9. Jouan-Lanhouet S, Riquet F, Duprez L, Vanden Berghe T, Takahashi N, Vandenabeele P. Necroptosis, in vivo detection in experimental disease models. *Semin Cell Dev Biol*. 2014;35:2-13.

10. Moriwaki K, Chan FK. Necroptosis-independent signaling by the RIP kinases in inflammation. *Cell Mol Life Sci*. 2016;73:2325-2334.

11. Lin J, Kumari S, Kim C, et al. RIPK1 counteracts ZBP1-mediated necroptosis to inhibit inflammation. *Nature*. 2016;540:124-128.

12. Wang Y, Wang H, Tao Y, Zhang S, Wang J, Feng X. Necroptosis inhibitor necrostatin-1 promotes cell protection and physiological function in traumatic spinal cord injury. *Neuroscience*. 2014;266:91-101.

13. Fan H, Tang HB, Kang J, et al. Involvement of endoplasmic reticulum stress in the necroptosis of microglia/macrophages after spinal cord injury. *Neuroscience*. 2015;311:362-373.

14. Kanno H, Ozawa H, Sekiguchi A, Itoi E. Spinal cord injury induces upregulation of Beclin 1 and promotes autophagic cell death. *Neurobiol Dis*. 2009;33:143-148.

15. Dong H, Fazzaro A, Xiang C, Korsmeyer SJ, Jacquin MF, McDonald JW. Enhanced oligodendrocyte survival after spinal cord injury in Bax-deficient mice and mice with delayed Wallerian degeneration. *J Neurosci*. 2003;23:8682-8691.

16. Kanno H, Ozawa H, Sekiguchi A, Yamaya S, Itoi E. Induction of autophagy and autophagic cell death in damaged neural tissue after acute spinal cord injury in mice. *Spine (Phila Pa 1976)*. 2011;36:E1427-E1434.

17. Huang J, Shang L, Zhang M, et al. Differential neuronal expression of receptor interacting protein 3 in rat retina: involvement in ischemic stress response. *BMC Neurosci*. 2013;14:16.

18. Roychowdhury S, McMullen M, Pisano S, Liu X, Nagy L. Absence of receptor interacting protein kinase 3 prevents ethanol-induced liver injury. *Hepatology*. 2013;57:1773-1783.

19. Lu J, Ashwell KW, Waite P. Advances in secondary spinal cord injury: role of apoptosis. *Spine (Phila Pa 1976)*. 2000;25:1859-1866.

20. Yong C, Arnold PM, Zoubine MN, et al. Apoptosis in cellular compartments of rat spinal cord after severe contusion injury. *J Neurotrauma*. 1998;15:459-472.

21. Citron BA, Arnold PM, Sebastian C, et al. Rapid upregulation of caspase-3 in rat spinal cord after injury: mRNA, protein, and cellular localization correlates with apoptotic cell death. *Exp Neurol*. 2000;166:213-226.

22. Liu XZ, Xu XM, Hu R, et al. Neuronal and glial apoptosis after traumatic spinal cord injury. *J Neurosci*. 1997;17:5395-5406.

23. Whalen M, Dalkara T, You Z, et al. Acute plasmalemma permeability and protracted clearance of injured cells after controlled cortical impact in mice. *J Cereb Blood Flow Metab*. 2008;28:490-505.

24. Vieira M, Fernandes J, Carreto L, et al. Ischemic insults induce necroptotic cell death in hippocampal neurons through the up-regulation of endogenous RIP3. *Neurobiol Dis*. 2014;68:26-36.

25. Qu Y, Tang J, Wang H, et al. RIPK3 interactions with MLKL and CaMKII mediate oligodendrocytes death in the developing brain. *Cell Death Dis*. 2017;8:e2629.

26. Ni Y, Gu WW, Liu ZH, et al. RIP1K contributes to neuronal and astrocytic cell death in ischemic stroke via activating autophagic-lysosomal pathway. *Neuroscience*. 2018;371:60-74.

27. Chen Y, Zhang L, Yu H, et al. Necrostatin-1 improves long-term functional recovery through protecting oligodendrocyte precursor cells after transient focal cerebral ischemia in mice. *Neuroscience*. 2018;371:229-241.

28. Smith YDM. Necroptosis, necrostatins and tissue injury. *J Cell Mol Med*. 2011;15:1797-1806.

29. Fan H, Zhang K, Shan L, et al. Reactive astrocytes undergo M1 microglia/macrohpages-induced necroptosis in spinal cord injury. *Mol Neurodegener*. 2016;11:14.

30. Grau JW, Huang YJ, Turtle JD, et al. When pain hurts: nociceptive stimulation induces a state of maladaptive plasticity and impairs recovery after spinal cord injury. *J Neurotrauma*. 2017;34:1873-1890.